Surface Modification of Ultrahigh Molecular Weight Polyethylene Fibers by Plasma Treatment. II. Mechanism of Surface Modification

SHANGLIN GAO[1,*] and YEGUANG ZENG[2]

[1]Testing Centre, Chongqing Institute of Architecture and Engineering, 630045, People's Republic of China; [2]Physics Department, Chongqing Teacher's College, 630047, People's Republic of China

SYNOPSIS

A detailed examination has been undertaken of the influence of surface treatment on the adhesion of ultrahigh molecular weight polyethylene (UHMW-PE) fibers to epoxy resin. XPS, SEM, FTIR–ATR, LRS, and contact-angle measurements have been used to characterize the chemical and physical changes of the fibers. The results, taken together, suggest that the adhesion depends on three factors: (i) chemical bonding effects, after plasma treatment, with the introduction of various kinds of oxygen-containing groups into the surface of the nonpolar polyethylene, which greatly improve the surface energy of the fibers; (ii) mechanical keying effects; and (iii) the nonpolar dispersion force. It is concluded that these three factors can be regarded as additive and the contributions from each of them to fiber/resin adhesion are different and change with increasing treatment time. The optimum results are obtained when their respective contribution reaches about 60%, 30%, and 10%. © 1993 John Wiley & Sons, Inc.

INTRODUCTION

The fiber–matrix interface or interphase has become the focus of attention recently.[1] Much information is now available about its chemistry and macrostructure.[2-5] The properties of the fiber/resin interface in ultrahigh molecular weight polyethylene (UHMW-PE) fiber/epoxy composites can play a dominant role in governing the overall performance of the interface.[6] Understanding the interactions occurring at the interface and being able to tailor them to give a desired composite property are of great importance.

The fiber/epoxy resin adhesion has been greatly reinforced by plasma treatment on UHMW-PE fibers.[7] Several other treatments for improving the adhesion and wettability properties of the polyethylene fibers or films have been studied and have met with varying degrees of success.[8-12] However, no one seems to have given a comprehensive summing-up of the mechanism of modification of surface adhesion, especially, a quantative analysis of the applied forces influencing interfacial adhesion.

The aim of the present work is to determine the changes of the surface and inner structure of the UHMW-PE fibers by plasma treatment and the influence on adhesion of each of the following factors: (i) the chemical-bonding effects; (ii) the mechanical interlocking; and (iii) the nonpolar dispersion force.

EXPERIMENTAL

Surface Spectroscopies

XPS gives information about the variation of concentration over the fiber surface.[13] Spectra of the untreated and plasma-modified samples were recorded on an ESCA LAB MKII spectrometer using MgK$\alpha_{1,2}$ ($h\gamma$ = 1253.6 eV) radiation. Binding energies are quoted to an accuracy of ±0.2 eV and area ratios, determined from curve-fitting procedures using a DuPont 310 Analogue Curve Resolver, to an accuracy of ±5%.

FTIR–ATR was performed using a Nicolet 5DXC FTIR spectrometer, using germanium internal re-

* To whom correspondence should be addressed.

Journal of Applied Polymer Science, Vol. 47, 2093–2101 (1993)
 CCC 0021-8995/93/122093-09

flection element (IRE) and a 45° incidence angle. Laser Raman spectra were obtained using a TOBIN YVON Laser Raman spectroscopy (LRS), the laser power on the sample was kept to 2 mW to avoid overheating the filaments, and the frequencies were 600–3200 cm^{-1}.

Measurements of Depth of Pits

There was a decrease in the mechanical properties of the fibers after plasma etching. This can be explained as the decrease in the effective area of the forces applied. Nardin and Ward used the following equation to indicate the relationship of the depth of pits[14]:

$$e = \frac{d}{2}\left[1 - \left(\frac{\sigma_p}{\sigma_0}\right)^{1/2}\right] \quad (1)$$

where d is the fiber diameter, and σ_p and σ_0 are, respectively, the tensile strengths of pitted and unpitted fibers.

To obtain satisfactory values, many tensile strength tests were conducted. Moreover, this equation is no longer valid for a filament with a cross section that is not perfectly circular. Therefore, we transform this equation through a simple deduction, if the initial Young's moduli of pitted and unpitted filaments are designated E_p and E_0, respectively, which were determined by a stress–strain instrument. Thus, e is given by

$$e = \frac{(a+b)}{4} - \frac{1}{2}\left[\frac{(a-b)^2}{4} + ab\frac{E_p}{E_0}\right]^{1/2} \quad (2)$$

where a and b are the lengths of major and minor axes of the cross section of the filament, respectively, i.e., the value of e was determined from measurements of E_p, E_0, a, and b.

Both calculations of the mean depth e of the pits do not take into account the stress concentration factor, which depends on both the depth and the tip radius of the pits.[14] The value of e calculated through these equations is therefore likely to be larger than the true value. However, provided that the tip radius of pits is constant, the calculations of e should provide satisfactory relative values for the damaged depth of plasma-treated samples.

Full details of the experimental material, plasma treatment, SEM, and surface energies by contact-angle measurements can be found in Part I of this work.[7] Here, it will suffice to say that the UHMW-PE monofilaments with draw ratios of 10.0, 29.0, 35.8, and 39.3 were used and that the term "fiber" appears without mentioning its draw ratio; this refers to the highest draw ratio material, in which the greatest scientific and technological interests lie.

RESULTS AND DISCUSSION

Effect of Plasma Treatment on Wetting Properties

The surface energy of the UHMW-PE fibers increases after plasma treatment from 34 mJ m^{-2} to about 60 mJ m^{-2} (cf. Fig. 1). It is far greater than that of the liquid epoxy resin (43 mJ m^{-2}), i.e., the treated fibers became completely wettable. As a result of plasma treatment, surface energy γ_s and its polar component γ_s^p increased greatly, yet the change in its dispersion component γ_s^d is small; therefore, the increase in γ_s is dependent on the increase in γ_s^p.

As shown in Figure 1, the surface energy increases rapidly with treatment time and reaches a plateau within 2 min. The surface energy of higher draw ratio fibers is a little greater than that of the lower draw ratio ones; therefore, the wettability of the higher draw ratio fibers should be better and more favorable to the fiber/resin adhesion. These results are in agreement with the relationship between the adhesion and plasma treatment time for different draw ratio fibers that was discussed in the first part of this work.[7]

Figures 2 and 3 show the effect of power and gas pressure of plasma treatment and their relation between the surface energy. The value of the surface

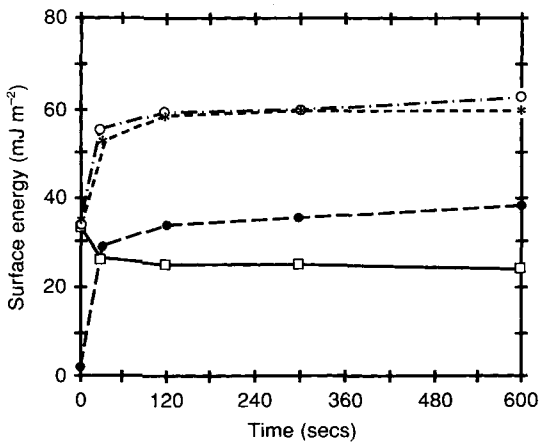

Figure 1 Surface free energy of monofilaments vs. mean plasma treatment time. (○) γ_s, (●) γ_s^p, and (□) γ_s^d are the surface free energy of monofilaments with draw ratio 39.3, (*) γ_s is the surface free energy of monofilaments with draw ratio 29.0 (67 W, 0.03 Torr).

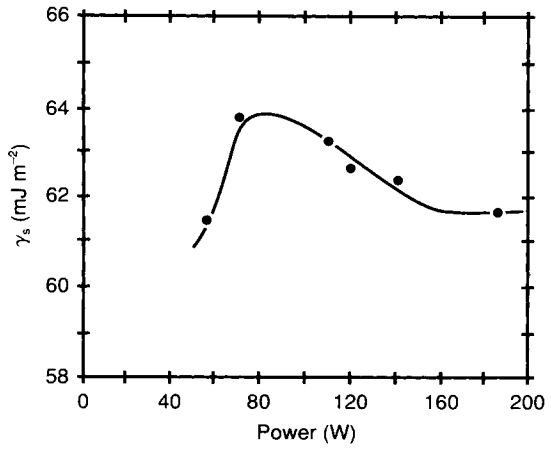

Figure 2 Surface free energy vs. mean power of plasma treatment for treated samples (300 s, 0.13 Torr).

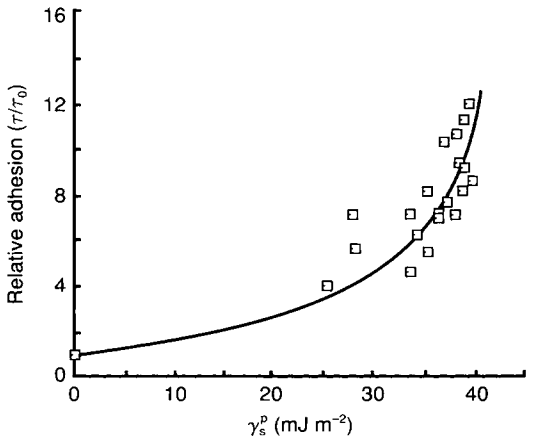

Figure 4 Polar component of the surface free energy in relation to relative adhesion of untreated and treated monofilaments.

energy is optimum under the treatment of 70–100 W and 0.1–0.2 Torr. This is also in agreement with the fact that the highest values of adhesion are obtained under the same treatment conditions.[7]

To observe more clearly the influence of surface energy on the adhesion, we plotted the adhesion against the polar component of surface energy for different draw ratio fibers and for different plasma treatment conditions (Fig. 4). It can be seen that the greater the γ_s^p the higher the adhesion. However, SEM observations show that the treated fiber surfaces are heavily pitted (cf. "Surface Texture" section below). Therefore, mechanical effects may influence the adhesion and a linear relationship between τ and γ_s^p would not be expected. This is indeed the case (Fig. 4), although the effect is partly hidden by the rapid increase of τ when γ_s^p tends to high values.

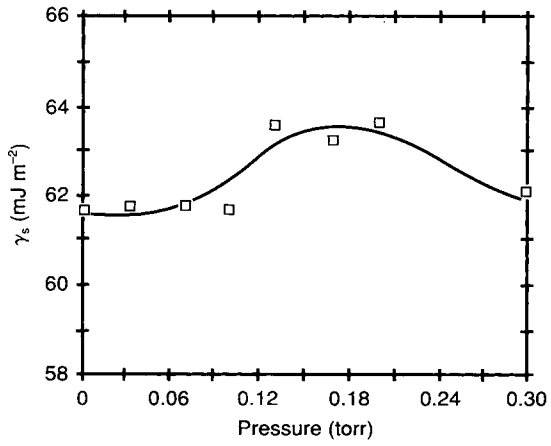

Figure 3 Surface free energy vs. mean gas pressure of plasma treatment (300 s, 67 W).

Changes in Surface Chemistry

XPS was used to monitor the introduction of functional groups and changes in surface chemistry produced by plasma treatment. A layer about 50 Å thick is observed.[15]

The great reactivity of UHMW-PE toward an oxygen or air plasma is evident from the C_{1s} spectra shown in Figure 5. The spectra from the plasma-treated samples consist of additional chemically shifted species 0.9–5.5 eV from the main peak. Similar −1.5 eV chemical shifts are obtained for O_{1s} spectra. Detailed analysis of the C_{1s} line profiles (cf. Fig. 5 and Table I) enabled components owing to carbons in $-\overset{|}{\underset{|}{C}}H$ (285.0 eV), $-\overset{|}{\underset{|}{C}}OH$ (286.2 eV), $=C=O$ (288.1 eV), $-COOH$ (289.4 eV), and $O=\overset{/}{C}-O-$ (290.5 eV) environments to be identified. Assignment of the peaks of the curve-fitted C_{1s} spectra were made on the basis of the studies over carbon fiber by Youxian.[16]

The air plasma-treated fiber surface contains only about 0.9% nitrogen (Table I), which is far less than that of the oxygen-containing groups; it is therefore the oxygen-containing groups that act as the main factor to affect the fiber/resin adhesion. Comparing the oxygen component groups after 600 s oxygen treatment with that after air plasma treatment (Table I), we found that the contents of $-COH$ after the two different treatments show little difference, but that a great difference lies mainly in the contents of the more active oxygen-containing groups, i.e., $=C=O$, $-COOH$, and $O=\overset{/}{C}-O-$ This

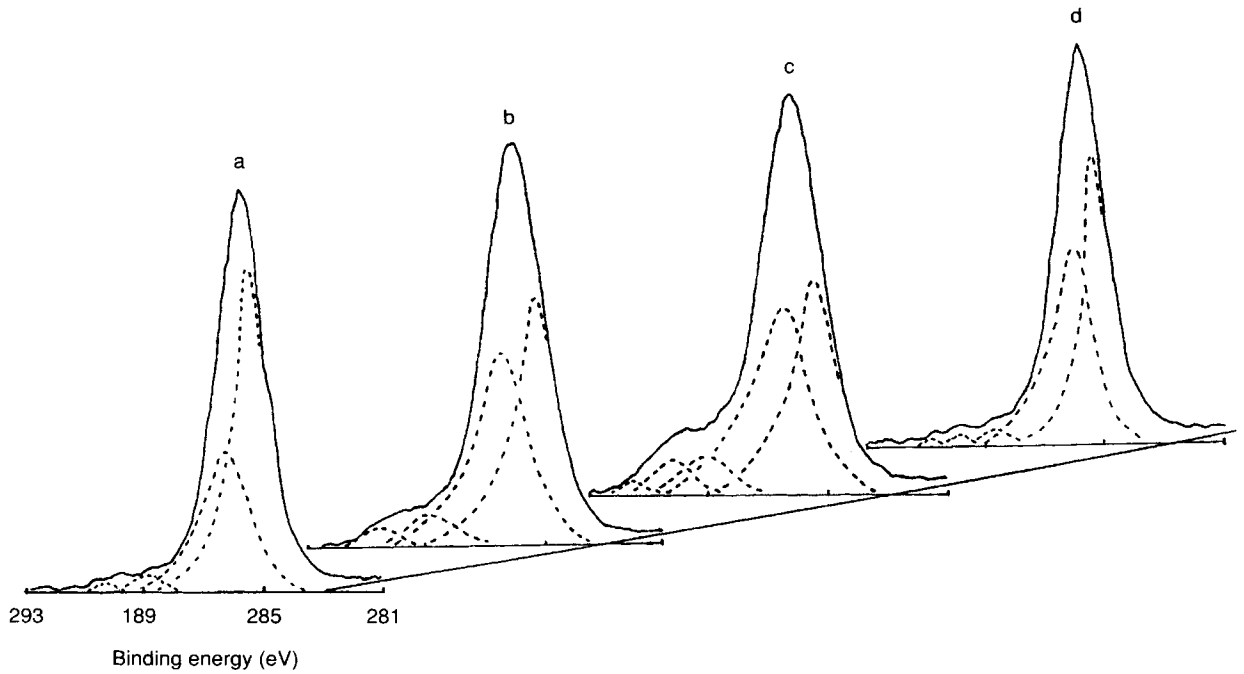

Figure 5 The C_{1s} spectra of UHMW-PE monofilaments. The curves have been fitted by computer: (a) untreated sample; (b) treated by oxygen plasma for 120 s; (c) treated by oxygen plasma for 600 s; (d) treated by air plasma for 600 s.

shows that the oxygen plasma treatment is more chemically efficient in creating oxygen-containing functional groups on the polyethylene surface.

For oxygen plasma-treated fiber, the —COH content on the fiber surface has increased by 11.5% from 26.1% to 37.6%, whereas the total content of $=C=O$, —COOH, and $O=\overset{/}{C}-O-$ showed a greater increase, i.e., 13.5% (from 2.8 to 16.3%). Though the —COH content on untreated fibers is high enough (i.e., 26%, it may be that this is because the surface was oxygenated when the fiber was formed), the fiber/resin adhesion is still poor. It is therefore likely that keto-, —COOH, and $O=\overset{/}{C}-O-$ groups are more effective in promoting adhesion than is the OH group.

Comparing the result of the fibers of different draw ratios that underwent the same treatment (Table I), we find that there are more oxygen-containing groups and oxygen content in fibers of higher draw ratio. This result is consistent with the conclusions that the higher the draw ratio, the higher the surface energy and the greater the adhesion.[7]

The groups' intensity changes as a function of treatment time resulting from the analysis (Table I) are shown in Figure 6. The concentration of all kinds of oxygen-containing groups increases with time and reaches a steady level very quickly. In contrast, that of CH group decreases greatly.

As discussed above, it appears that the plasma (oxygen) treatment is chemically very efficient in increasing the immediate surface concentration of functional groups and may help to increase the number of chemical bonds between fiber and resin. In Figure 7, a plot of results for fiber/resin adhesion as a function of C_{1s}/O_{1s} ratio is shown together with a fitted curve. The fiber bondability increases with the increase of the oxygen content and thus causes the increase of the adhesion.

In comparison of the similar types of the relationships of C_{1s}/O_{1s} ratio and γ_s^p with τ/τ_0 (Figs. 4 and 7), both emphasize the importance of the chemical bonding factor on the fiber/resin adhesion. However, mechanical effects are partly hidden by the rapid increase of τ/τ_0 when γ_s^p and O_{1s}/C_{1s} ratio tends to high values. As shown in Figures 1 and 6, the dramatic change in surface chemistry vs. treatment time is also reflected in the increase of γ_s^p with treatment time. Therefore, as we expected, a linear relationship is obtained between the C_{1s}/O_{1s} ratio and γ_s^p (Fig. 8). Hence, the big increase of γ_s^p is accompanied by a change in chemistry.

The Laser Raman and FTIR–ATR spectrometers

Table I XPS Data for Surface Composition of UHMW-PE Monofilaments

D.R.	Time (s)	Gas	Content (%) C/O	N	C	O	O_{1s} (eV) E_b	Relative Content	N_{1s} (eV) E_b	Relative Content
39.3	0		11.0		91.7	8.3	532.8	2800		
	120	O_2	5.1		83.5	16.5	534.3	7100		
	600	O_2	3.0		75.2	24.3	534.3	8200		
	600	Air	5.2	0.9	83.0	16.0	534.2	5500	402.0	410
10.0	0		14.8		93.7	6.3	532.9	2100		
	300	O_2	5.4		84.3	15.7	534.3	5200		
	600	O_2	6.9		87.4	12.6	534.3	4800		

—C—H		—C—OH		C_{1s} (eV) =C=O		—COOH		—C—O— ‖ O	
E_b (eV)	Content (%)	E_b (eV)	Content (%)	E_b (eV)	Content (%)	E_b (eV)	Content (%)	E_b (eV)	Content (%)
285.0	71.1	285.9	26.1	288.1	2.0	288.5	0.8		
285.0	58.6	286.2	32.1	288.2	5.2	289.5	2.8	290.5	1.2
285.2	46.2	286.3	37.6	288.2	8.6	289.4	5.4	290.6	2.3
285.0	62.2	286.2	30.3	288.1	4.6	289.4	2.4	290.5	0.6
285.0	73.4	286.0	24.7	288.2	1.4	289.1	0.5		
285.1	55.4	286.0	33.9	288.1	7.4	289.5	3.1	290.3	0.2
285.1	53.6	286.1	36.4	288.0	7.2	289.4	2.2	290.2	0.6

allow us to observe a thicker layer[17] (LRS, 1–2 μm; FTIR-ATR, 0.3–0.8 μm). However, as expected, there are no signals of chemistry changes being detected. The spectra reflect only the inner structure of the fibers. This arises because plasma treatment alters only a very thin layer (about 20 Å), and the concentration is only of the order of a few μmol/g. It can be concluded that the plasma treatment allows the chemistry of the fiber surface to be altered without the reaction penetrating deep into the fiber, thus avoiding too much damage and allowing the retention of beneficial mechanical properties.

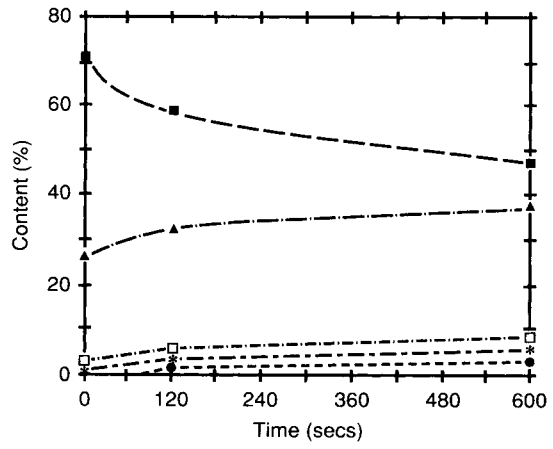

Figure 6 Relationship between C_{1s} contents of different active groups on the monofilaments (D.R. 39.3) surface and the time of oxygen plasma treatment: (■) —C—H; (▲) —C—OH; (□) =C=O; (*) —COOH; (●) —O—C=O.

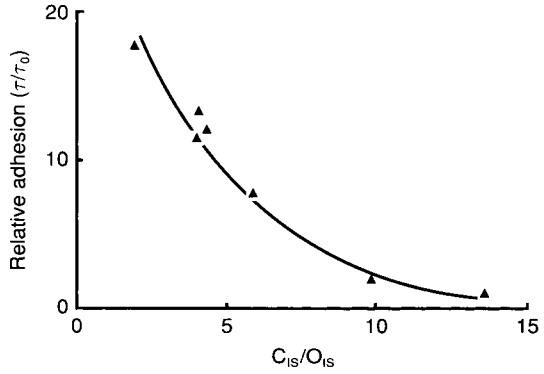

Figure 7 Pull-out relative adhesion τ/τ_0 vs. mean C_{1s}/O_{1s} intensity ratio for monofilaments.

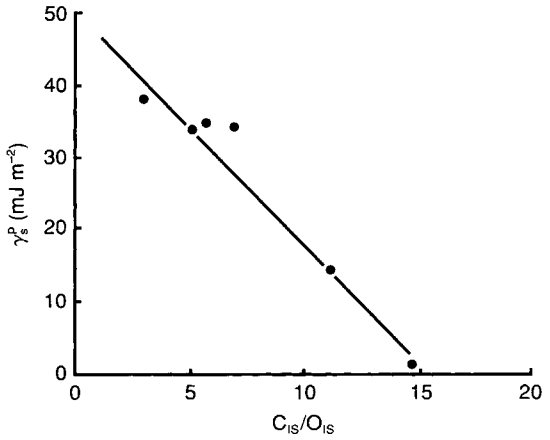

Figure 8 Relationship between polar component of surface free energy γ_s^p and C_{1s}/O_{1s} intensity ratio for plasma-treated and untreated surfaces of monofilaments.

The Effect of Plasma Treatment on Surface Texture

A scanning electron micrograph of an untreated fiber is shown in Figure 9 (a). It can be seen that the surface is fairly smooth, except for longitudinal striations that indicate the possible presence of fibrils.[11]

Plasma treatment produces a dramatic change, as shown in Figure 9 (b), (c), and (d). A highly developed cellular and rhombic structure has now replaced the longitudinal striations, with pits varying in diameter and depth in the range 0.5–5 μm. The pits were caused by the degradation of the molecule chains on the fiber surface as a result of plasma etching and reaction overheating. These pits result in a great increase of the surface area and, thus, provide more favorable conditions for various physical and chemical interactions between fiber and resin.

Of plasma-treated fibers, the remarkable cellular surface structure, into which resin can penetrate to produce a mechanical interlocking between fiber and resin, is one of the most important factors in improving the fiber/resin adhesion.

As found previously, it can be observed that the pit size of fiber with a higher draw ratio is bigger than that of the lower one[11] [Figs. 9 (c) and (d)].

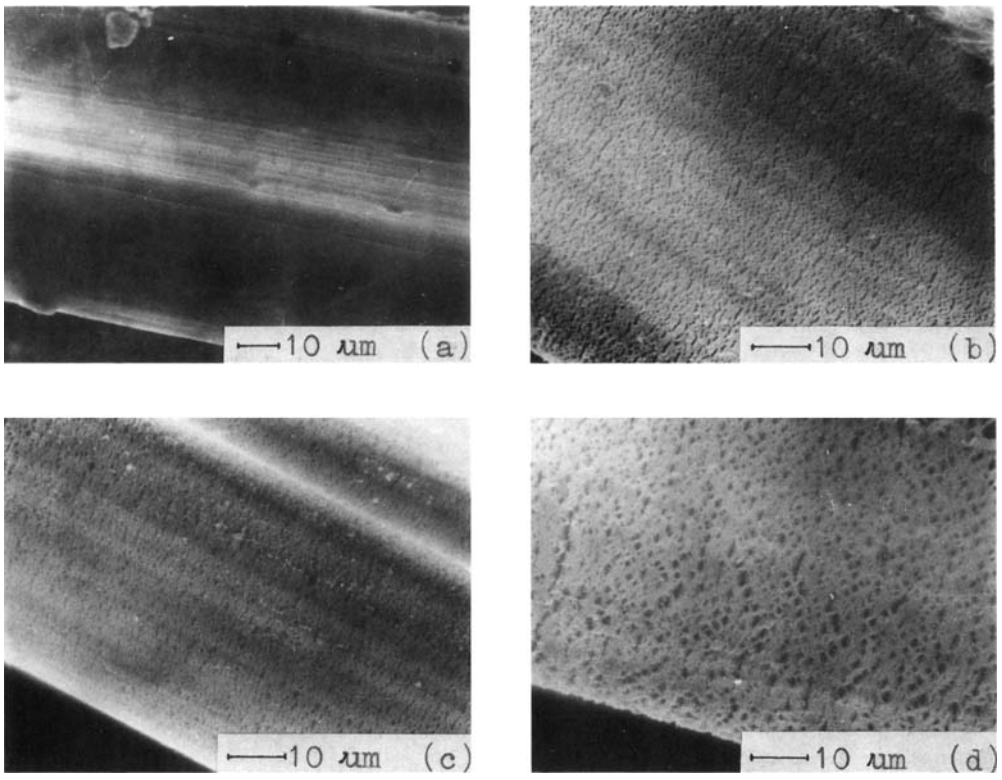

Figure 9 SEM micrographs: (a) and (b) untreated and treated (600 s) fibers of draw ratio 39.3, respectively; (c) and (d) fibers with draw ratios 10.0 and 35.8 after 300 s plasma treatment, respectively.

The increase in the pit size with increasing draw ratio allows a more effective keying between resin and fiber, and the peel-off proceeds deeper inside the fiber as the draw ratio increases. In addition, the increase in tensile strength of the fibrils with increasing draw ratio will be accompanied by a higher failure load for the pullout system.

Next, we evaluate quantitively the mean depth e of the pits using eq. (2). The variation of e with treatment time, power, and pressure is shown in Figure 10. It can be seen that the mean depth of the pits increases rapidly within the first 120 s treatment time, then the value of e increases slowly, with its maximum at 300 s. This is similar to the variation of the γ_s^p and τ/τ_0 with the treatment time (cf. Fig. 1 here and Fig. 3 in Ref. 7). The difference lies in the rates of γ_s^p, e, and τ/τ_0 reaching their plateau values with the increase of time, at which γ_s^p is the fastest, while e is the slowest and τ/τ_0 is between the two. It therefore implys that the increase of τ/τ_0 is the result of the combined contribution from the chemical bonding and mechanical keying.

As shown in Figure 10 also, the effect of power on the depth of pits was very dramatic; it suggests that the UHMW-PE fibers are better treated with lower power to prevent its mechanical properties from decreasing too much. The effect of gas pressure on the depth of the pits is insignificant.

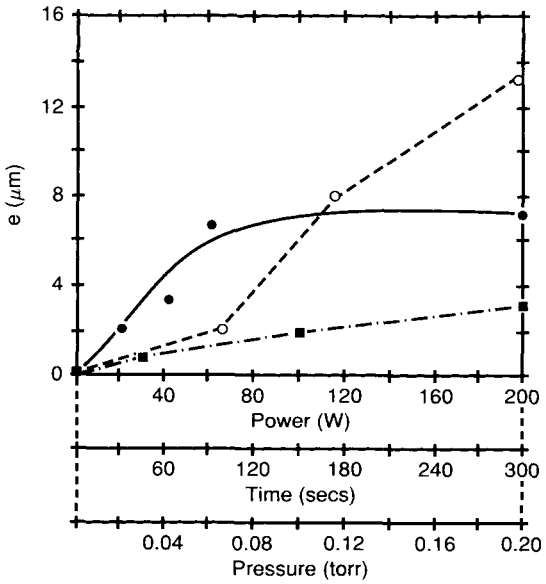

Figure 10 Relationship between depth of pits and (○) plasma treatment power, (●) time, and (■) pressure for treated samples. The smooth curve is a fitted one according to the theory to be discussed in the following content.

A Quantitative Analysis on the Contributions from the Factors Affecting the Fiber/Resin Adhesion

From the foregoing discussions, we sum up the factors affecting the fiber/resin adhesion as follows: the interface chemical bonding, the mechanical interlocking, and the nonpolar dispersion.

To clarify the contributions, respectively, of the three factors to the adhesion, we use $\tau(t)$ to indicate the fiber/resin adhesion for a certain period of plasma treatment time. $\tau_c(t)$, $\tau_m(t)$, and $\tau_d(t)$ are, respectively, the components of the adhesion for the chemical bonding, mechanical interlocking, and nonpolar dispersion. Their quantitative relation is

$$\tau(t) = \tau_c(t) + \tau_m(t) + \tau_d(t) \tag{3}$$

As shown in Figure 8, the increase of the oxygen-containing groups is linear with the increase of the polar component of surface energy γ_s^p. The role that the chemical bonding, caused by the oxygen-containing groups, plays in the fiber/resin adhesion can be represented by

$$\tau_c(t) = k_c \gamma_s^p(t) \tag{4}$$

where k_c is constant.

The mechanical interlocking is caused by the gearing interface with the resin penetrating into the pits. Its strength is influenced by the depth the resin embeds in the pits, and it is also affected by the size of the pits and the draw ratio of the fiber. e^n is therefore used to indicate the effect the pits have on mechanical interlocking, and the experimental date will be fitted to determine the value of n. $\tau_m(t)$ is given by

$$\tau_m(t) = k_m e^n(t) \tag{5}$$

where $e(t)$ is the mean depth of the pits after a certain period of plasma treatment time; k_m stands for the coefficient concerning the draw ratios of the fibers.

The nonpolar dispersion is less strong compared with the above two factors and is assumed to be least affected by plasma treatment, i.e., $\tau_d(t) = \tau_d(0)$ = constant. Since $e(0) \approx 0$, $\gamma_s^p(0) \approx 0$. According to eqs. (3)–(5), the fiber/resin adhesion of the untreated fibers is

$$\tau_0 = \tau(0) = \tau_d(0) = \tau_d(t) \tag{6}$$

Combining eqs. (4)–(6) with (3), we get

$$\frac{\tau(t)}{\tau_0} - 1 = \frac{k_m}{\tau_0} e^n(t) + \frac{k_c}{\tau_0} \gamma_s^p(t) \tag{7}$$

The theoretical value of $e(t)$ is given by

$$e(t) = \left\{ \left[\frac{\tau(t)}{\tau_0} - 1 - \frac{k_c}{\tau_0} \gamma_s^p(t) \right] \cdot \frac{\tau_0}{k_m} \right\}^{1/n} \tag{8}$$

As shown in Table II and Figure 10, $\tau(300)/\tau_0 = 7.6$, $e(300) = 7.2$ μm, $\gamma_s^p(300) = 35.5$ mJ m^{-2}, $\tau(30)/\tau_0 = 4.9$, $e(30) = 2.2$ μm, and $\gamma_s^p(30) = 28.5$ mJ m^{-2}. Substituting them into eq. (7), we get the values of k_m/τ_0 and k_c/τ_0 for different values of n, respectively. Then, the theoretical lines obtained from eq. (8) are plotted together with the experimental values of e. In this case, a reasonable fit was obtained for value of $n = 2$ (see Fig. 10 and Table II).

Furthermore, the contributions from chemical bonding, mechanical interlocking, and nonpolar dispersion to the fiber/resin adhesion are, respectively, evaluated by the following equations:

$$\frac{\tau_c(t)}{\tau(t)} = \frac{k_c}{\tau_0} \cdot \frac{\tau_0}{\tau(t)} \cdot \gamma_s^p(t) \tag{9}$$

$$\frac{\tau_m(t)}{\tau(t)} = \frac{k_m}{\tau_0} \cdot \frac{\tau_0}{\tau(t)} \cdot e^2(t) \tag{10}$$

$$\frac{\tau_d(t)}{\tau(t)} = \frac{\tau_0}{\tau(t)} \tag{11}$$

The result of above equations is given in Figure 11. It can be seen that the greatest contribution to the adhesion is from the chemical bonding, which accounts for over 60%. $\tau_c(t)/\tau(t)$ achieves its extreme value (76%) within 30 s treatment time.

The contribution from mechanical interlocking accounts for about 30%. It gradually increases with the increase of treatment time and reaches the extreme value at 300 s. It should be noted that the contribution from mechanical interlocking increases with the fiber draw ratio, because fibers of higher draw ratio are of higher shear strength and have comparatively bigger plasma-etched pits. Thus, it can be seen that reinforcing the shear strength of fiber surface is one way to improve the fiber/resin adhesion.

Table II $\tau(t)/\tau_0$, γ_s^p, and e [calculated by eq. (8), $n = 2$] vs. Mean Time of Plasma Treatment

Time (s)	$\tau(t)/\tau_0$	γ_s^p (mJ m^{-2})	e (μm)
30	4.90	28.5	2.20
60	5.75	31.8	3.99
90	6.25	33.2	4.92
120	6.60	33.8	5.59
180	7.05	34.1	6.49
240	7.35	34.7	6.93
300	7.60	35.5	7.20

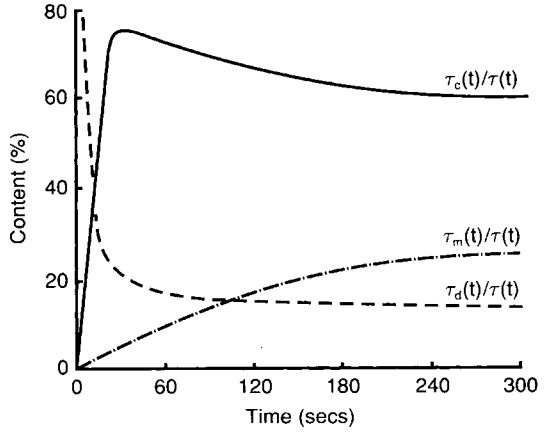

Figure 11 The roles $\tau_c(t)$, $\tau_m(t)$, and $\tau_d(t)$ play in the fiber/resin adhesion as a function of plasma treatment time.

In contrast to the chemical bonding and mechanical interlocking, the contribution from nonpolar dispersion sharply decreases to about 10% when it reaches the plateau value with the increasing treatment time.

From the above analysis, we can tell the locus of failure of PE/epoxy joint shifted with different treatment time (see Part I of this work, Fig. 5). When the treatment time is short (within 60 s), the effect of mechanical interlocking is not significant and chemical bonding plays a crucial role in the adhesion; however, its effect is not strong enough to peel off the entire treated PE layer.

When the treatment time reaches 300 s, the effect of mechanical interlocking and the degree of peel-off become great due to the increase of pits size. The entire treated PE layer is peeled off.

Because of the decrease of the mechanical properties of the fiber surface and a layer of deposition resulting from long time treatment, a weak boundary layer between fiber and resin was formed, along which the interface failure slides, and such a layer causes the decrease of peel-off; hence, τ_m and τ.

Moreover, the reason for the relationship between τ/τ_0 and γ_s^p (or C_{1s}/O_{1s}) being a curve rather than

a linear (Figs. 4 and 7) is that the mechanical keying effect became more and more significant with the increasing values of γ_s^p (or O_{1s}/C_{1s}).

CONCLUSIONS

The wettability of the UHMW-PE fibers has been improved after plasma treatment, thus meeting the prerequisite of the fiber/resin adhesion. Various kinds of oxygen-containing groups are introduced into the fiber surface and resulted in the increase of the polar component of the surface energy. The plasma-etched pits are found in the fiber surface. This causes the mechanical interlocking with the resin embedded in the pits.

The fiber/resin adhesion $\tau(t)$ can be considered as the sum of three shear strength terms, which relate, respectively, to chemical bonding $\tau_c(t)$, mechanical interlocking $\tau_m(t)$, and nonpolar dispersion $\tau_d(t)$. $\tau_e(t)$ is directly related to the surface concentration of oxygen-containing groups; it is also related to the polar component of the surface energy: The two are approximately in linear with each other. $\tau_m(t)$ is linear with the square of $e(t)$; it is also affected by the draw ratios of the fibers. The plasma treatment has little influence on $\tau_d(t)$.

The contributions from $\tau_c(t)$, $\tau_m(t)$, and $\tau_d(t)$ to fiber/resin adhesion are significantly different and vary with the increasing of treatment time. At a treatment time of 300 s, the optimum results of $\tau(t)$ are obtained when the contribution from each of them are, respectively, 61%, 26%, and 13%.

The authors wish to thank Dr. L. H. Duan, Institute of Physics, Academia Sinica, for providing the testing instruments and Mr. Q. W. Mau for technical assistance with these instruments. We are indebted to Prof. C. T. Yuan and C. Guo for useful discussions and invaluable support during the course of this project.

REFERENCES

1. M. R. Piggott, *Comp. Sci. Tech.*, **42,** 57 (1991).
2. R. J. Young, C. Galiotis, I. M. Robinson, and D. N. Batchelder, *J. Mater. Sci.*, **22,** 3642 (1987).
3. S. Holmes and P. Schwertz, *Comp. Sci. Tech.*, **38,** 1 (1990).
4. M. R. Piggott, *Comp. Sci. Tech.*, **42,** 57 (1991).
5. C. Tones, *Comp. Sci. Tech.*, **42,** 275 (1991).
6. S. L. Gao and Y. G. Zeng, Paper presented at the Meeting of Advances in Polymeric Matrix Composites, American Chemical Society, San Francisco, CA, April 5–10, 1992.
7. S. L. Gao and Y. G. Zeng, *J. Appl. Polym. Sci.*, **47,** 2065 (1993).
8. A. R. Postema, A. T. Doorn Kamp, J. G. Meijer, H. v. d. Vlekkert, and A. J. Pennings, *Polym. Bull.*, **16,** 1 (1986).
9. I. M. Ward and N. H. Ladizesky, *Pure Appl. Chem.*, **57,** 1641 (1985).
10. H. D. Wagner and D. A. Cohn, *Biomaterials*, to appear.
11. N. H. Ladizesky and I. M. Ward, *J. Mater. Sci.*, **18,** 533 (1983).
12. D. M. Brewis, *J. Mater. Sci.*, **3,** 262 (1968).
13. D. T. Clark and D. R. Hutton, *J. Polym. Sci. Polym. Chem. Ed.*, **25,** 2643 (1987).
14. M. Nardin and I. M. Ward, *Mater. Sci. Tech.*, **3,** 814 (1987).
15. D. T. Clark, W. J. Feast, W. K. R. Musgrave, and I. Ritchie, *J. Polym. Sci. Chem. Ed.*, **13,** 857 (1975).
16. D. Youxian, *Comp. Sci. Tech.*, **30,** 119 (1987).
17. F. M. Mirabella, *Appl. Spectrosc. Rev.*, **21,** 45 (1985).

Received December 10, 1991
Accepted May 14, 1992